World Academy of Science, Engineering and Technology
International Journal of Chemical and Molecular Engineering
Vol:8, No:12, 2014

Numerical Study of Vortex Formation inside a Stirred Tank

Divya Rajavathsavai, Akhilesh Khapre, Basudeb Munshi

***Abstract*—**The computational fluid dynamics (CFD) study of stirred tank with the air-water interface are carried out in the presence of different types of the impeller and with or without baffles. A multiple reference frame (MRF) approach with the volume of fluid (VOF) method is used to capture the air-water interface. The RANS (Reynolds Averaged Navier-Stokes) equations with *k-ε* turbulence model are solved to predict the flow behavior of water and air phase which are treated as a different phases. The predicted results have shown that the VOF method is able to capture the interface in the unbaffled tank. While, the VOF method is showing an unfeasible results in the baffled tank with high rotational impeller speed. For continuous stirred tank, the air-water interface is disturbed by the inflow and the level of water is also increased with time.

***Keywords*—**Computational Fluid Dynamics, stirred tank, air-water interface, multiple reference frame, volume of fluid, Reynolds Averaged Navier-Stokes equations.

I. Introduction

STIRRED tank reactors usually contain different types of baffles, like four flat vertical plates that either mounted on or offset from the tank wall to avoid vortex formation and the air entrainment within the reactor. The presence of baffles enhances mixing process effectively. However, the tanks without baffles are also important in several tank applications like crystallization and precipitation, solid-liquid mass transfer, fermentation, solid suspension and many more. A huge amount of experimental and computational fluid dynamic modelling work on the hydrodynamics and mixing in the baffled tanks agitated mostly by Rushton turbines and also other agitators types has been reported in the literature. But, a very limited number of experimental and computational studies have been carried out in the unbaffled tanks [1]. Nagata [2] determined velocity profiles in a flat bottom unbaffled cylindrical tank with co-axial turbine agitator. The Reynolds number used to carry out the experiment was in the order of 105. In most experimental studies, the top liquid surface was covered with a lid to avoid vortex formation and air entrainment.

Numerical simulations of turbulent free surface flows in the unbaffled tanks are scant. Ciofalo et al. [3] developed an iterative method to determine the vortex shape. The technique involved with an initial guess of the free surface profile, which assumed as a flat. The free surface profile used to generate body fitted computational mesh. The flow field and surface pressure using different RANS turbulence models were calculated on the generated body fitted mesh. The surface pressure used to compute the new shape of the liquid surface. The method is computationally inexpedient as it requires a generation of the new mesh for the next iteration. Hence, the use of VOF method for capturing gas-liquid interface is more convenient option. The VOF method for CFD was first applied by Serra et al. [4] to simulate flows with wavy free surface in the baffled tanks.

Haque et al. [5] coupled VOF method with a homogeneous multiphase CFD model. It was used first time to simulate turbulent flows with a liquid surface in the unbaffled tank, which is agitated by a paddle impeller and Rushton turbine. The predicted vortex profiles generated by both impellers using the free surface models were compared with the experimentally determined profiles by Nagata [2] and Ciofalo et al. [3]. Torre et al. [6] used Eulerian-Eulerian multiphase approach with VOF method along with *k-ε* and Reynolds Stress Transport (RST) turbulence models to capture the vortex shape and the air entrainment. The simulation was done in a partially baffled tank agitated by a retreat curve blade impeller. The numerical prediction of the free surface shape was in good agreement with experimental data. Lamarque et al. [7] simulated a complex turbulent free surface flow in an unbaffled mixing tank using Large-eddy Simulation. The free surface vortex generation was captured using a front tracking method. The fluid was agitated by a magnetic rod in place of a classical mixing device such as paddle or propeller impellers.

The objective of this study is to simulate mixing tank with different types of impellers at different axial position, and capture the interface between air and water phase. The computed values of the vortex height are compared with the theoretically computed values [8]. The simulation of vortex formation study in continuous stirred tank reactor is also carried out to see the evolution of vortex height with time.

II. Numerical Details

A. Geometry Specification

A flat bottom unbaffled stirred tank is taken for the computational simulation of air-water multiphase system. The density and viscosity of water used for simulation are 998.2 kg/m^3 and 0.001 kg/m·s respectively. Similarly for air the density is 1.225 kg/m^3 and viscosity is 1.785x10^{-5} kg/m·s. The diameter (*D*) of tank is 0.2m. The height of tank is extended to

Divya Rajavathsavai and Basudeb Munshi are with the National Institute of Technology, Rourkela, Orissa, 769008, India.

Akhilesh Khapre is with National Institute of Technology, Rourkela, Orissa, 769008, India (corresponding author phone: +91-7894044869; e-mail: akhilesh_khapre@yahoo.co.in).

1.5*D* in order to give a sufficient space for the elevation of water along the tank wall surface. Two different types of impeller, Rushton turbine and paddle impeller are used for stirring the water. The diameter of both the impellers (d_m) is *D*/3.Two different positions; *D*/3 and *D*/4 are used to mount the impeller above the bottom surface of stirred tank. The computational domain of the stirred tank is discretized using an unstructured mesh consisting of near about 200000 tetrahedral elements (Fig. 1). At rest position the height of liquid is maintained at 0.2m above the bottom of tank.

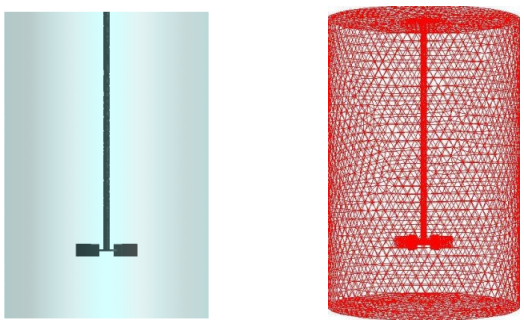

(a) (b)

Fig. 1 (a) computational tank domain, (b) computational mesh

B. Governing Equations and Solution Procedure

The general conservation of mass or continuity equation can be written as follows [9],

$$\frac{\partial \rho}{\partial t} + \nabla .(\rho \vec{v}) = 0 \tag{1}$$

where, $\vec{v}$ is the velocity vectors.

The VOF formulation in ANSYS FLUENT is usually used to calculate a time-dependent solution. But for the problems with a steady-state solution, it is possible to carry out a steady-state calculation, provided a solution is independent of initial guess. In case of vortex formation system with liquid-gas interface, the solution depends on the initial liquid height and hence transient solution method should be chosen [9].

The VOF formulation depends on the fact that two or more phases are not interpenetrating. For each control volume, the volume fractions of all phases must be total to unity. The fields for all variables and properties are shared by the phases and represent volume-averaged values, providing that the volume fraction of all the phases is well-known at every location. Thus, the variables and properties in any known cell are either only characteristic of one of the phases or a mixture of the phases, as it depends upon the volume fraction values. In different words, if the q^{th} fluid's volume fraction within the cell is indicated as α_q, then the following three conditions are possible [9]:

$\alpha_q = 0$: The cell is empty (of the q^{th} fluid).

$\alpha_q = 1$: The cell is full (of the q^{th} fluid).

$0 < \alpha_q < 1$: The cell contained interface between the q^{th} fluid and one or more other fluid.

Based on the local value of α_q, the appropriate properties and variables is assigned to each control volume within the computational domain.

The tracking of the interface between the phases is done by the solution of a continuity equation for the volume fraction of one or more of the phases. For the q^{th} (fluid's volume fraction) phase, the equation is written as [9]

$$\frac{1}{\rho_q}\left[\frac{\partial}{\partial t}(\alpha_q \rho_q) + \nabla .(\alpha_q \rho_q \vec{v}_q) = S_{\alpha_q} + \sum_{p=1}^{n}\left(\dot{m}_{pq} - \dot{m}_{qp}\right)\right] \tag{2}$$

where, $\dot{m}_{qp}$ is the mass transfer from phase q to phase p and $\dot{m}_{pq}$ is the rate of mass transfer from phase p to phase q. By default, the source term on the right-hand side of equation, S_{α_q}, is zero, but can specify a constant or user-defined mass source for each phase.

The volume fraction equation will not be solved for the primary phase; the primary-phase volume fraction will be computed based on the following constraint:

$$\sum_{p=1}^{n} \alpha_q = 1 \tag{3}$$

The properties appearing in the transport equations are determined by the presence of the component phases in each control volume. In a two-phase system, for example, if the phases are represented by the subscripts 1 and 2, and the mixture density in each cell is given by [9]

$$\rho = \alpha_2 \rho_2 + (1 - \alpha_2)\rho_1 \tag{4}$$

In general, for n phase system, the volume-fraction-averaged density takes on the following form:

$$\rho = \sum \alpha_q \rho_q \tag{5}$$

All other properties (e.g., viscosity) are also computed in this manner.

A single momentum equation is solved throughout the computational domain, and the resulting velocity field is shared among the phases. The momentum equation, shown below, is dependent on the volume fractions of all phases through the properties ρ and μ [9],

$$\frac{\partial}{\partial t}(\rho \vec{v}) + \nabla .(\rho \vec{v}\vec{v}) = -\nabla p + \nabla .\left[\mu\left(\nabla \vec{v} + \nabla \vec{v}^{T}\right)\right] + \rho \vec{g} + \vec{F} \tag{6}$$

where, p is the static pressure, $\vec{g}$ and $\vec{F}$ are the gravitational body force and external body forces respectively.

The turbulence kinetic energy, k, and its rate of dissipation, ε, are predicted by the equations [9],

$$\frac{\partial}{\partial t}(\rho k)+\nabla\cdot(\rho k\vec{v})=\nabla\cdot\left[\left(\mu+\frac{\mu_t}{\sigma_k}\right)\nabla\cdot k\right]+G_k-\rho\varepsilon \quad (7)$$

and

$$\frac{\partial}{\partial t}(\rho\varepsilon)+\nabla\cdot(\rho\varepsilon\vec{v})=\nabla\cdot\left[\left(\mu+\frac{\mu_t}{\sigma_\varepsilon}\right)\nabla\cdot\varepsilon\right]+C_{1\varepsilon}\frac{\varepsilon}{k}G_k-C_{2\varepsilon}\rho\frac{\varepsilon^2}{k} \quad (8)$$

where G_k represents generation of turbulent kinetic energy and the model constant have the following default values,

$$C_{1\varepsilon}=1.44, C_{2\varepsilon}=1.92, C_\mu=0.09, \sigma_k=1.0, \sigma_\varepsilon=1.3 \quad (9)$$

The unbaffled stirred tank is modelled using a multiple reference frame (MRF) and VOF method for capturing the air-water interface. In MRF approach, the impeller and shaft are kept stationary while the tank wall and bottom surface are assigned an angular velocity which is equal and opposite of the impeller rotational speed. No-slip boundary condition is applied to all solid walls. At the top wall of the tank, zero-shear boundary condition is used. The Reynolds Averaged Navier-Stokes (RANS) equations are solved to obtain the velocity flow field inside the tank. The realizable k-ε turbulence model with a standard wall function is used to resolve the turbulence created by a moving impeller. The PISO algorithm is used for coupling the pressure and velocity. For the simulations which are carried out using the transient solver, the implicit first order scheme in time and the second order upwind difference scheme for convective and turbulent terms are used. The convergence criteria for all discretized terms are set to the order of 10^{-3}.

III. Results and Discussion

The simulation is carried out at four different impeller rotational speeds, 100, 200, 300 and 400 rpm. The impeller Reynolds number for each rotational speed is in the turbulent region. The contours of the water phase in Figs. 2 and 3 show the predicted profiles of air-water interface obtained using VOF method in the stirred tanks for both Rushton turbine and paddle impeller with bottom clearance of $D/3$. The figures show that as the rotating speed of impeller increases, the depth of air-water interface also increases. At impeller rotational speed of 400 rpm, the air-water interface level is well below the impeller mounting position. Table I draws the comparison of theoretical vortex height with the predicted air-water interface from the simulation. The theoretical vortex height is taken from literature [8]. The predicted air-water interface is calculated by subtracting the final position of the interface from the initial position that is 0.2m.

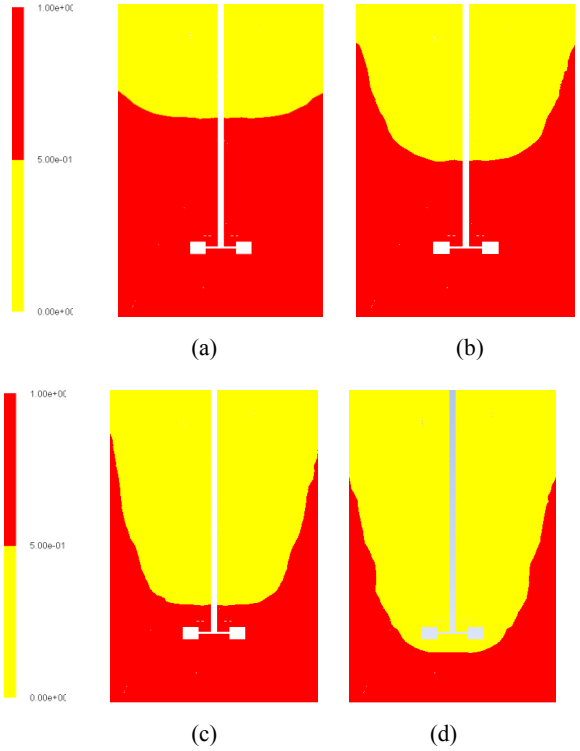

Fig. 2 Predicted air-water interface in stirred tank agitated by Rushton turbine with bottom clearance of $D/3$, (a) 100rpm, (b) 200 rpm, (c) 300 rpm, (d) 400 rpm

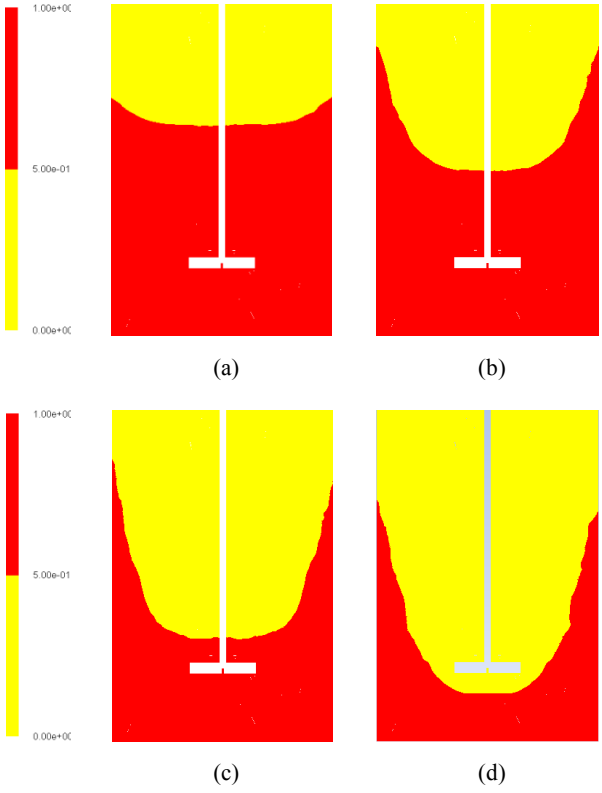

Fig. 3 Predicted air-water interface in stirred tank agitated by Paddle impeller at bottom clearance of $D/3$, (a) 100rpm, (b) 200 rpm, (c) 300 rpm, (d) 400 rpm

TABLE I
COMPARISON OF AIR-WATER INTERFACE HEIGHT BETWEEN THEORETICAL AND PREDICTED VALUES WITH IMPELLER CLEARANCE *D*/3

Impeller Rotation (RPM)	Theoretical vortex height value [8]	Predicted air-water interface value at clearance *D*/3 of impeller (in mm)	
		Rushton turbine	Paddle impeller
100	4.12	9.1	10.1
200	16.48	50.4	50.8
300	37.08	106.3	106.3
400	65.93	152.7	156.7

Figs. 4 and 5 show the predicted profiles of air-water interface for both types of impeller Rushton turbine and paddle impeller with bottom clearance of *D*/4 for impeller rotational speed ranging from 100 to 400 rpm. The comparison of theoretical vortex height with the predicted air- water interface for the impeller with bottom clearance of *D*/4 can be seen in Table II

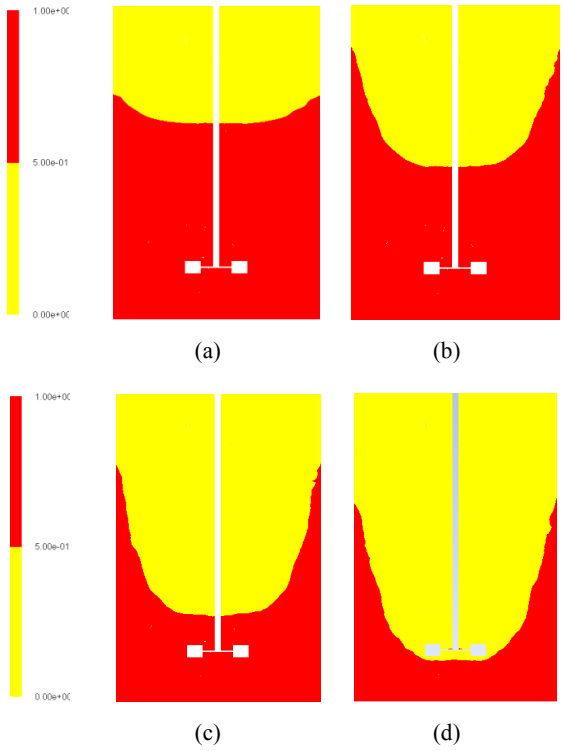

(a) (b)

(c) (d)

Fig. 4 Predicted air-water interface in stirred tank agitated by Rushton turbine at bottom clearance of *D*/4

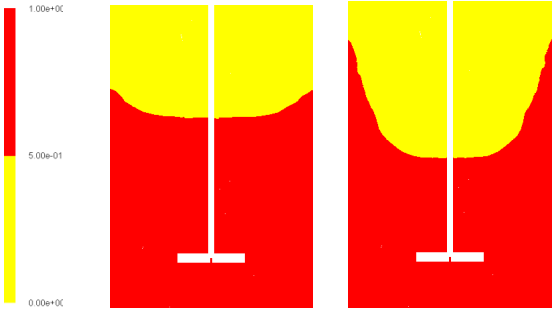

(a) b)

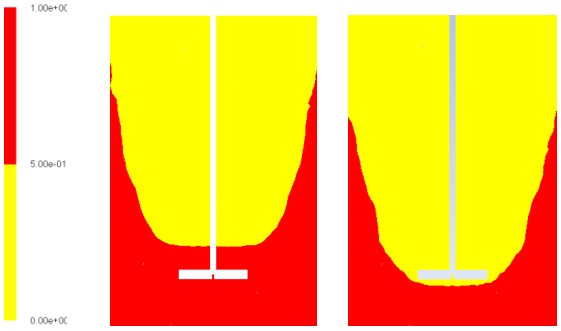

(c) (d)

Fig. 5 Predicted air-water interface in stirred tank agitated by Paddle impeller at bottom clearance of *D*/4

TABLE II
COMPARISON OF AIR-WATER INTERFACE HEIGHT BETWEEN THEORETICAL AND PREDICTED VALUES WITH IMPELLER CLEARANCE *D*/4

Impeller Rotation (RPM)	Theoretical vortex height value [8] (in mm)	Predicted air-water interface value at clearance *D*/4 of impeller (in mm)	
		Rushton turbine	Paddle impeller
100	4.36	12.7	11.9
200	17.44	54.3	53.5
300	39.26	116.2	122.7
400	69.79	148.7	161.4

From both Tables I and II, it is clear that the predicted values of air-water interface by VOF method is found very large compared to the theoretical values of it. The values predicted are almost double the theoretical values.

The velocity vector plots for both Rushton and paddle impellers at different rotational speed of impeller with bottom clearance of *D*/3 are shown in Figs. 6 and 7. The vector planes are shown at the impeller disk level that is at *D*/3 distance from the bottom tank wall. The same natures of velocity vector profiles are obtained for the impeller with bottom clearance of *D*/4. It is observed in Figs. 6 and 7 that water is set to a circulatory motion due to rotation of impeller in the absence of baffles in the tank. The velocity magnitude increases with the increasing rotational speed of the impeller. The highest magnitude of the velocity is found near to the tank wall. This is because of the simulation strategy adapted to solve the problem where the impeller and shaft are kept constant and the wall of the tank is assigned to angular rotation speed.

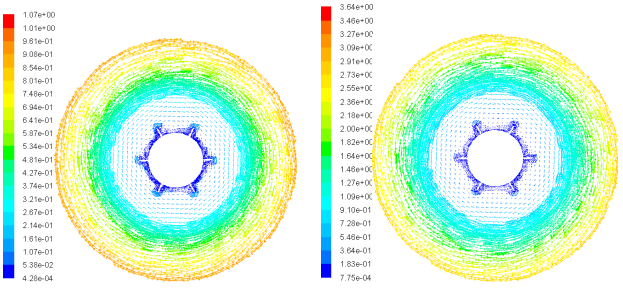

(a) (b)

Fig. 6 Velocity vector plots for Rushton turbine mounted at clearance of *D*/3, (a) 100rpm, (b) 400 rpm

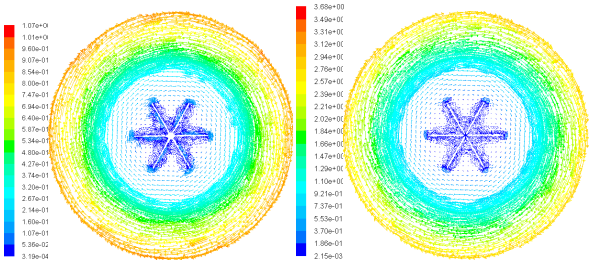

(a) (b)

Fig. 7 Velocity vector plots for paddle impeller mounted at clearance of *D*/3, (a) 100rpm, (b) 400 rpm

The air-water interface in continuous unbaffled stirred tank with the Rushton turbine mounted at clearance of *D*/3 is also shown in Fig. 8. It represents the effect of the inlet flow on the air-water interface. The diameter of inlet and outlet pipe is taken as 0.01m. The inlet pipe is mounted at height of 0.22m above the bottom surface of the tank, and outlet pipe is mounted near the bottom of the tank. The tank is simulated till a steady state with inlet and outlet flow equal to zero. This is considered as the time equal to zero. The vortex is formed at steady state, and then inlet flow rate with 0.5 m/s velocity starts to flow. Figs. 8 (b) and (c) show the effect of inlet flow on the interface at time 5 sec and 10 sec after the water starts to flow continuously in the tank. The smooth shape of the interface is interrupted by the inlet flow. After 10 seconds, the interface is completely destroyed and the water level is observed to increase with time.

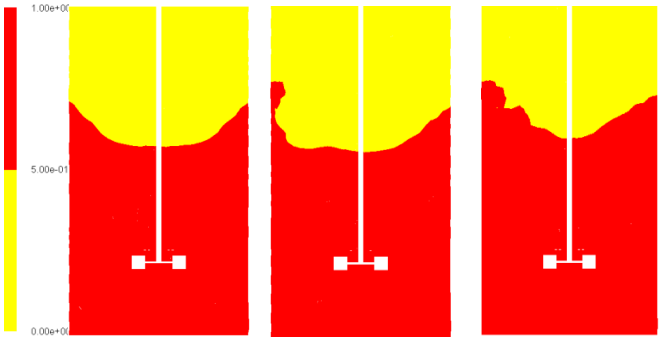

(a) At 0 sec (b) at 5 sec (c) at10 sec

Fig. 8 Effect of inlet flow on air-water interface in continuous stirred tank

The air-water interface study is furthermore carried out for the baffled stirred tank with Rushton turbine mounted at clearance of *D*/3. The width of baffle is taken as *D*/10. The simulation is carried out using the same strategy as in a case of the unbaffled stirred tank. Fig. 9 shows the comparison between the air-water interfaces (in terms of water phase fraction) formed in a stirred tank in absence and presence of baffles with impeller rotating at 100 rpm. Fig. 10 depicts the iso-surface of interface in both stirred tank. The interface formed in the unbaffled tank is smooth and uniformed in nature (Fig. 10 (a)). While the interface formed in the baffled tank showed the little deep level of interface behind each baffle (Fig. 10 (b)). This might be due to the formation of secondary circulation behind the baffles. The simulation for higher rotational speed of the impeller in the baffled tank has also carried out, but it showed physically an unfeasible results.

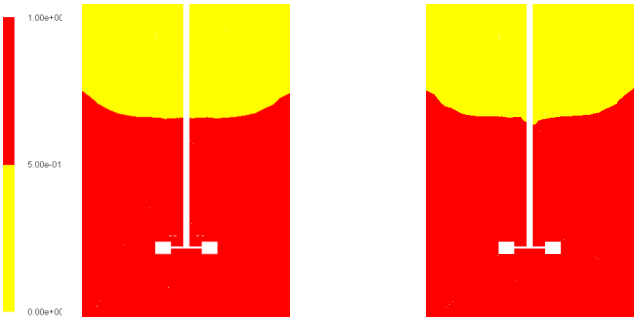

(a) Unbaffled tank (b) Baffled tank

Fig. 9 Comparison of air-water interface in unbaffled and baffled stirred tank

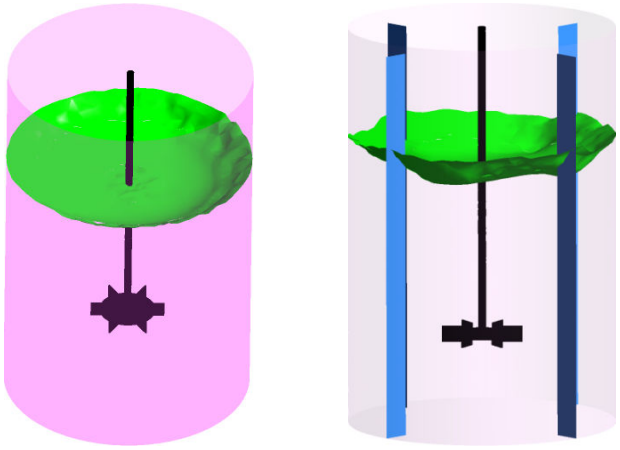

(a) (b)

Fig. 10 Iso-surface comparison of interface in (a) unbaffled tank, (b) baffled tank showing deep level of interface behind baffle

IV. Conclusions

The simulation of stirred tank with air-water multiphase system is done. The air-water interface is captured using Volume of Fluid (VOF) method. The simulation results are able to capture the interface in the unbaffled tank. But in the baffled case with high impeller rotational speed, it showed an unfeasible result. As the rotational speed of impeller is increased, the level of the air-water interface is moved towards the impeller. For impeller speed of 400 rpm, the air-water interface level is reached well below the impeller position and the air is entrained into the impeller region. In continuous stirred tank, the inflow water disturbed the air-water interface and also the water level is increased with time.

References

[1] T. Mahmud, J. N. Haque, K. J. Roberts, D. Rhodes and D. Wilkinson, "Measurements and modelling of free-surface turbulent flows induced

by a magnetic stirrer in an unbaffled stirred tank reactor", Chemical Engineering Science, vol. 64, pp. 4197–4209, 2009.
[2] S. Nagata, Mixing Principles and Applications, Wiley, New York, 1975.
[3] M. Ciofalo, A. Brucato, F. Grisafi and N. Torraca, "Turbulent flow in closed and free-surface unbaffled tanks stirred by radial impeller", Chemical Engineering Science, Vol. 51, pp. 3557–3573, 1996.
[4] A. Serra, M. Campolo and A. Soldati, "Time dependent finite-volume simulation of the turbulent flow in a free-surface CSTR", Chemical Engineering Science, Vol. 56, pp. 2715–2720, 2001.
[5] J. N. Haque, T. Mahmud, K. J. Roberts and D. Rhodes, "Modeling turbulent flows with free-surface in unbaffled agitated vessels", Industrial and Engineering Chemistry Research, Vol. 45, pp. 2881–2891, 2006
[6] J. Torré, D. F. Fletcher, T. Lasuye and C. Xuereb, "Single and multiphase CFD approaches for modelling partial baffled stirred vessels: Comparison of experimental data with numerical predictions", Chemical Engineering science, Vol. 62, pp. 6246–6262, 2007
[7] N. Lamarque, B. Zoppe, O. Lebaigue, Y. Dolias, M. Bertrand and F. Ducros, "Large-eddy simulation of the turbulent free-surface flow in an unbaffled stirred tank reactor", Chemical Engineering Science, Vol. 65, pp. 4307–4322, 2010.
[8] M. Zlokarnik, "Trombentiefebeimrühren in unbewehrtenbehältern", ChemieIngenieurTechnik, Vol. 43, pp.1028–1030, 1971.
[9] ANSYS FLUENT 12.0 Theory Guide, Chapter 16: Multiphase Flow, ANSYS, Inc., 2009.